Dalton
www.rsc.org/dalton

Heterobimetallic complexes with dppm-bridged Ru/Pd, Ru/Pt, Ru/Au and Ru/Cu centers

Ying Yang, Khalil A. Abboud and Lisa McElwee-White*
Department of Chemistry and Center for Catalysis, University of Florida, Gainesville, FL, 32611-7200, USA. E-mail: lmwhite@chem.ufl.edu; Fax: +1 352 846 0296; Tel: +1 352 392 8768

Received 14th July 2003, Accepted 5th September 2003
First published as an Advance Article on the web 23rd September 2003

The heterobimetallic Ru/Pd, Ru/Pt, Ru/Au and Ru/Cu complexes $Cp(PPh_3)Ru(\mu\text{-}I)(\mu\text{-}dppm)PdCl_2$ (**4**), $Cp(PPh_3)Ru(\mu\text{-}Cl)(\mu\text{-}dppm)Pd(CH_3)Cl$ (**5**), $Cp(PPh_3)Ru(\mu\text{-}I)(\mu\text{-}dppm)PtCl_2$ (**6**), $Cp(PPh_3)Ru(\mu\text{-}I)(\mu\text{-}dppm)PtI_2$ (**7**), $Cp(PPh_3)RuI(\mu\text{-}dppm)AuI$ (**8**), $Cp(PPh_3)RuBr(\mu\text{-}dppm)AuCl$ (**9**), $Cp(PPh_3)RuCl[\mu\text{-}PPh_2(CH_2)_4PPh_2]AuCl$ (**10**), $Cp(PPh_3)RuCl(\mu\text{-}Ph_2PNHPPh_2)AuCl$ (**11**) and $Cp(PPh_3)Ru(\mu\text{-}I)(\mu\text{-}dppm)CuI$ (**12**) were prepared by the reactions of $CpRu(PPh_3)(\eta^1\text{-}Ph_2PQPPh_2)X$ [$Q = (CH_2)_n$ (n = 1, 4), NH; X = Cl, Br, I, Me] with $Pd(COD)Cl_2$, $Pt(COD)Cl_2$, $Pt(COD)I_2$, $Au(PPh_3)Cl$, AuI, AuCl and CuI, respectively. The structures of compounds **4**, **5**, **10** and **12** were determined by X-ray crystallography. Cyclic voltammetry of the halide-bridged complexes revealed shifts in the redox potentials of the metals, as compared to mononuclear model compounds. The shifts are consistent with electron donation between the metals through the halide bridge. Ru/Au complexes **8**–**11**, which are bridged only by the bidentate phosphine, exhibited minimal electronic effects between the metal centers. This limited interaction between the metal centers in **8**–**11** is corroborated by UV/vis spectroscopy.

Introduction

Heterobimetallic systems have been of interest in the context of homogeneous catalysis due to the possibility that the different metal centers could exhibit cooperative behavior.[1–7] Each metal could play a unique mechanistic role[8] or such effects could be the result of one metal center mediating the reactivity of another.[9,10] Our interest in the possibility of such cooperative effects between metal centers during homogenous electrooxidation of alcohols led us to prepare the heterobimetallic complexes $Cp(PPh_3)Ru(\mu\text{-}Cl)(\mu\text{-}dppm)PdCl_2$ (**1**),[11] $Cp(PPh_3)Ru(\mu\text{-}Cl)(\mu\text{-}dppm)PtCl_2$ (**2**)[12] and $Cp(PPh_3)RuCl(\mu\text{-}dppm)AuCl$ (**3**).[11] Cyclic voltammetry of complexes **1**–**3** in the presence of methanol led to significant enhancement of oxidative currents, consistent with a catalytic process.[11–13] Bulk electrolysis of methanol in the presence of the heterobimetallic complexes resulted in much higher current efficiencies than those obtained from the mononuclear model compound $CpRu(\eta^2\text{-}dppm)Cl$ (**13**), suggesting that the second metal center enhances catalytic activity.

Although all three bimetallic complexes (**1**–**3**) show enhanced activity as compared to Ru, Pd, Pt and Au model compounds, the metal–metal interactions differ. Complexes **1** and **2** both possess a bridging chloride that links the metal centers in a distorted six-membered ring. Cyclic voltammetry of **1** and **2** demonstrated shifts in the formal wave potentials of Ru(II/III), Pd(II/IV) and Pt(II/IV) redox couples relative to the model compounds, indicating significant electron donation through the chloride bridge from Ru to the electron deficient Pd and Pt centers. In contrast, the redox potentials of the Ru(II/III) and Au(I/III) couples in **3** resemble those of their mononuclear model compounds, suggesting a minimal interaction between the two metal centers *via* the bridging dppm ligand. In order to further explore these metal–metal interactions and the resulting catalytic activity, an extended series of compounds with ligands of varying electronic character has now been prepared.

In this work, we report the synthesis and characterization of additional Ru/Pd, Ru/Pt, Ru/Au and Ru/Cu heterobimetallic complexes that are similar to **1**–**3**, but exhibit systematic perturbations in the ancillary ligands. These new compounds provide a series of related species for study of cooperative effects between the two metal centers. Alcohol oxidation studies using these compounds as electrocatalysts will be reported in due course.

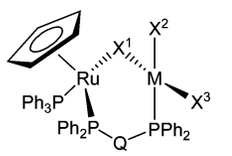

Compound	M	X^1	X^2	X^3	Q
1	Pd	Cl	Cl	Cl	CH_2
2	Pt	Cl	Cl	Cl	CH_2
4	Pd	I	Cl	Cl	CH_2
5	Pd	Cl	Cl	Me	CH_2
6	Pt	I	Cl	Cl	CH_2
7	Pt	I	I	I	CH_2

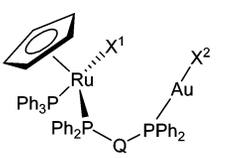

Compound	X^1	X^2	Q
3	Cl	Cl	CH_2
8	I	I	CH_2
9	Br	Cl	CH_2
10	Cl	Cl	$(CH_2)_4$
11	Cl	Cl	NH

Results and discussion

Synthesis

Synthesis of Ru/Pd complexes 4 and 5. Ru/Pd complex **1** was previously prepared by reaction of $CpRu(PPh_3)(\eta^1\text{-}dppm)Cl$ (**14**) with $Pd(COD)Cl_2$ in CH_2Cl_2 at room temperature.[11] The I-bridged Ru/Pd complex **4** was prepared as a red powder in an analogous manner from $CpRu(PPh_3)(\eta^1\text{-}dppm)I$ (**16**) and $Pd(COD)Cl_2$ (Scheme 1). In contrast, reaction of $CpRu(PPh_3)(\eta^1\text{-}dppm)Me$ (**17**) with $Pd(COD)Cl_2$ in benzene at room temperature afforded the Pd–Me complex **5** in 90% yield. Transfer of the methyl group from Ru to Pd resulted in formation of the Cl-bridged core structure seen in heterobinuclear complex **1**. Complexes **4** and **5** are air stable in their solid states and do not show signs of decomposition in solution even when exposed to air for days.

DOI: 10.1039/b307990b

 This journal is © The Royal Society of Chemistry 2003

Table 1 NMR data for complexes **1**–**19**[a]

	^{1}H NMR (δ)		^{31}P NMR (δ)			
	Cp	Q	Ru–PPh_3	Ru–PPh_2	M–PPh_2	Ref.
1	4.72	2.67 (m)	37.5 (d, 35 Hz)	52.2 (dd, 28, 35 Hz)	19.7 (d, 28 Hz)	11
2	4.67	2.78 (m)	37.8 (d, 36 Hz)	49.1 (dd, 21, 36 Hz)	−2.9 (d, 20 Hz)	12,13
3	4.09	4.74 (m), 1.33 (m)	42.8 (d, 43 Hz)	36.3 (dd, 28, 43 Hz)	20.8 (d, 28 Hz)	11
4	4.65	3.48 (m), 2.72 (m)	40.1 (dd, 7, 35 Hz)	49.5 (dd, 20, 35 Hz)	10.5 (dd, 7, 20 Hz)	[b]
5	4.58	2.86 (m)	39.3 (d, 36 Hz)	45.6 (dd, 36, 27 Hz)	25.5 (d, 27 Hz)	[b]
6	4.63	3.45 (m), 2.94 (m)	40.5 (dd, 3, 35 Hz)	46.4 (dd, 11, 35 Hz)	−7.7 (dd, 3, 11 Hz)	[b]
7	4.65	3.52 (m), 3.12 (m)	40.4 (dd, 3, 35 Hz)	45.8 (dd, 12, 35 Hz)	−2.1 (dd, 3, 12 Hz)	[b]
8	4.16	5.04 (m), 1.60 (m)	41.7 (d, 42 Hz)	31.4 (dd, 25, 42 Hz)	27.9 (d, 25 Hz)	[b]
9	4.12	4.86 (m), 1.43 (m)	42.5 (d, 42 Hz)	34.2 (dd, 27.5, 42 Hz)	22.0 (d, 27.5 Hz)	[b]
10	4.11	2.21–0.55 (m)	44.8 (d, 42 Hz)	37.0 (d, 42 Hz)	31.6 (s)	[b]
11	4.12	5.93 (m, NH)	54.0 (d, 38 Hz)	87.7 (dd, 46, 38 Hz)	40.4 (d, 46 Hz)	[b]
12	4.34	2.89 (m), 2.51 (m)	40.3 (d, 40 Hz)	26.7 (dd, 40, 20 Hz)	−18.5 (br s)	[b]
13	4.70	5.08 (m), 4.36 (m)		13.4 (s)		18
14	4.10	3.84 (m), 1.11 (m)	43.4 (d, 41 Hz)	37.5 (dd, 41, 20 Hz)	−28.4 (d, 20 Hz)	19
15	4.13	3.94 (m), 1.15 (m)	43.2 (d, 42 Hz)	35.8 (dd, 42, 20 Hz)	−27.5 (d, 20 Hz)	[b]
16	4.18	4.12 (m), 1.24 (m)	42.9 (d, 41 Hz)	33.5 (dd, 41, 20 Hz)	−27.0 (d, 20 Hz)	[b]
17	4.19	2.82 (m), 1.15 (m)	59.3 (dd, 3, 37 Hz)	48.2 (dd, 16, 37 Hz)	−27.8 (dd, 3, 16 Hz)	[b]
18	4.09	2.30–0.50 (m)	44.7 (d, 42 Hz)	37.3 (d, 42 Hz)	−14.4 (s)	[b]
19	4.11	4.82 (m, NH)	42.0 (d, 46 Hz)	85.5 (dd, 46, 12 Hz)	24.3 (d, 12 Hz)	[b]

[a] Spectra measured in $CDCl_3$ at room temperature. [b] This work.

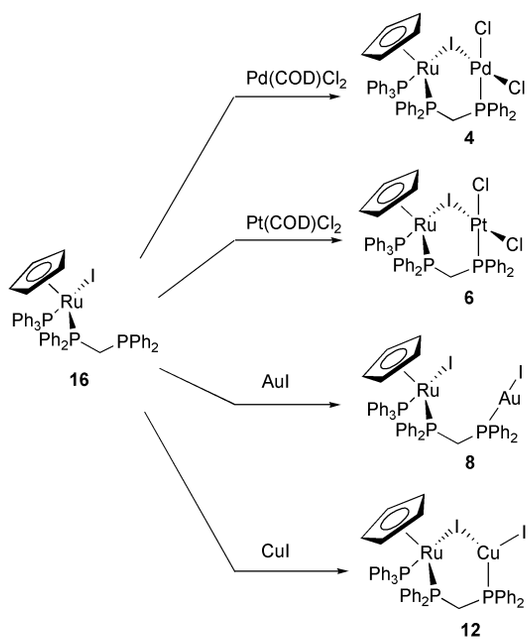

Scheme 1 Representative synthetic routes to the heterobimetallic complexes

Synthesis of Ru/Pt complexes 6 and 7. The reactions of Ru complex **16** with $Pt(COD)Cl_2$ and $Pt(COD)I_2$ in CH_2Cl_2 at room temperature afforded the I-bridged Ru/Pt complexes **6** and **7**, respectively (Scheme 1). Although a significant amount of $Pt(\eta^2\text{-dppm})Cl_2$ was formed by dppm transfer in the similar reaction of $CpRu(PPh_3)(\eta^1\text{-dppm})Cl$ (**14**) with $Pt(COD)Cl_2$ to make heterobimetallic complex **2**, no phosphine transfer to produce $Pt(\eta^2\text{-dppm})Cl_2$ or $Pt(\eta^2\text{-dppm})I_2$ occurred during preparation of **6** and **7**. The stabilities of complexes **6** and **7** are very similar to those of the Ru/Pd complexes **4** and **5** both in the solid state and in solution.

Synthesis of Ru/Au complexes 8–11. An equimolar ratio of the Ru complex **16** and AuI were reacted in CH_2Cl_2 at room temperature to afford the Ru/Au complex **8** as an orange powder in 97% yield (Scheme 1). Complex **8** has a structure similar to that of complex **3** but with the chlorides replaced by iodides. Complex **9** was prepared in the same manner as **3** starting from $CpRu(PPh_3)(\eta^1\text{-dppm})Br$ (**15**) and $Au(PPh_3)Cl$. The attempt to prepare complex **9** by the reaction of **15** and AuCl in CH_2Cl_2 at room temperature formed a mixture of products due to halide exchange between Br and Cl. The reaction of $CpRu(PPh_3)(\eta^1\text{-dppb})Cl$ (**18**) with AuCl in CH_2Cl_2 at room temperature resulted in the formation of the heterobimetallic Ru/Au complex **10**, in which the two metal centers are linked by a bridging dppb ligand. The Ru/Au complex **11**, in which the two metal centers are linked by a bridging $Ph_2P\text{-}NHPPh_2$ ligand, was synthesized in an analogous manner from $CpRu(PPh_3)(\eta^1\text{-}Ph_2PNHPPh_2)Cl$ (**19**) and AuCl. When $Au(PPh_3)Cl$ was used as the starting material for the syntheses of complexes **10** and **11**, a broad peak for the Au-bound phosphines was usually observed. The line broadening was ascribed to a coordination equilibrium at the Au center involving the triphenyl phosphine released during the reaction. Gold(I) complexes with one to four coordinated phosphine ligands have been detected in solution,[14–16] and these complexes are known to undergo facile ligand exchange.[15–17] Clean samples of complexes **10** and **11** with normal linewidths in their ^{31}P NMR spectra can be obtained from the reactions of $Au(PPh_3)Cl$ with **15** and **18**, respectively, but multiple recrystallizations of the products are necessary.

Synthesis of Ru/Cu complex 12. The heterobimetallic Ru/Cu complex **12** was prepared as a deep red powder by the reaction of **16** with excess CuI in CH_2Cl_2 at room temperature (Scheme 1). The compound is moderately stable in its solid state but decomposes slowly in solution when stored outside of a glove box.

NMR data

The $^{31}P\{^1H\}$ NMR spectrum of **5** (Table 1) exhibits the expected three resonances. The downfield resonances (45.6 and 39.3 ppm) correspond to the Ru-bound phosphines while the upfield doublet is assigned to the Pd-bound phosphorus of the bridging dppm. In the ^{1}H NMR spectrum of **5**, the Cp signal appears as a singlet at 4.58 ppm with the methyl group giving rise to a doublet at 0.39 ppm. The diastereotopic methylene protons of the bridging dppm are observed as a multiplet at 2.86 ppm as a result of coupling to the adjacent phosphorus atoms. The spectra of **4** are similar with the exception that an additional J_{PP} between the Pd-bound dppm phosphorus and Ru–PPh_3 can be observed in the $^{31}P\{^1H\}$ NMR spectrum, and

Table 2 Crystal data and structure refinement for complexes **4**, **5**, **10** and **12**

Complex	**4**	**5**	**10**	**12**
Empirical formula	$C_{52}H_{46}Cl_{14}IP_3PdRu$	$C_{55}H_{57}Cl_8P_3PdRu$	$C_{51}H_{48}AuCl_2P_3Ru$	$C_{50}H_{46}Cl_4CuI_2P_3Ru$
M_r	1594.47	1301.99	1122.74	1299.99
T/K	173(2)	173(2)	193(2)	193(2)
λ/Å	0.71073	0.71073	0.71073	0.71073
Crystal system	Triclinic	Monoclinic	Monoclinic	Monoclinic
Space group	$P\bar{1}$	$P2_1/n$	$P2_1/n$	$P2_1/n$
a/Å	11.4480(13)	13.8306(6)	13.7910(6)	20.2849(8)
b/Å	12.2567(14)	22.8974(9)	18.5416(8)	11.3392(5)
c/Å	22.402(3)	18.4161(7)	18.4876(8)	20.9410(9)
α/°	98.508(2)	90	90	90
β/°	96.142(2)	108.070(2)	109.800(2)	91.758(2)
γ/°	90.895(2)	90	90	90
V/Å^3	3089.2(6)	5544.4(4)	4447.9(3)	4814.5(4)
Z	2	4	4	4
D_c/Mg m^{-3}	1.714	1.560	1.677	1.793
μ/mm^{-1}	1.753	1.105	3.898	2.395
F_{000}	1568	2520	2224	2552
Crystal size/mm	0.17 × 0.15 × 0.10	0.36 × 0.24 × 0.23	0.23 × 0.23 × 0.07	0.19 × 0.17 × 0.11
θ Range/°	0.92 to 27.50	1.78 to 27.50	1.92 to 27.50	1.38 to 27.49
Index ranges	$-14 \le h \le 14$ $-15 \le k \le 15$ $-28 \le l \le 29$	$-13 \le h \le 17$ $-29 \le k \le 28$ $-23 \le l \le 23$	$-17 \le h \le 17$ $-23 \le k \le 24$ $-24 \le l \le 23$	$-26 \le h \le 26$ $-14 \le k \le 14$ $-27 \le l \le 26$
Reflections collected	26139	36509	39309	42538
Independent reflections (R_{int})	13243 (0.0389)	12593 (0.0352)	10148 (0.0551)	11042 (0.0392)
Completeness to $\theta = 27.49°$ (%)	93.5	98.9	99.5	99.8
Absorption correction	Integration	Integration	Analytical	Integration
Max./min. transmission	0.8572/0.7580	0.8300/0.6953	0.7741/0.3779	0.7944/0.6136
Data/restraints/parameters	13243/30/689	12593/0/505	10148/0/538	11042/0/553
GOF on F^2	1.072	1.007	1.051	1.041
$R1$ [a]	0.0582	0.0381	0.0386	0.0325
$wR2$ [b]	0.1298	0.0794	0.0747	0.0784
Largest diff. peak, hole/e Å^{-3}	1.827, −2.275	0.882, −1.874	1.572, −0.509	0.756, −0.473

[a] $R1 = \Sigma(||F_o| - |F_c||)/\Sigma|F_o|$ [b] $wR2 = [\Sigma[w(F_o^2 - F_c^2)^2]/\Sigma[w(F_o^2)^2]]^{1/2}$; $S = [w(F_o^2 - F_c^2)^2]/(n - p)]^{1/2}$; $w = 1/[\sigma^2(F_o^2) + (0.0337p)^2 + 1.24p]$; $p = [\max(F_o^2,0) + 2F_c^2]/3$.

the chemical shifts of the diastereotopic methylene protons differ significantly, with two multiplets appearing at 3.48 and 2.72 ppm.

The $^{31}P\{^1H\}$ NMR spectra of **6** and **7** both exhibit three resonances as expected (Table 1). The downfield Ru-bound phosphorus signals of the two complexes are quite similar, while the upfield ones assigned to the Pt-bound phosphorus atoms exhibit a chemical shift difference of 5.6 ppm due to the different halide ligands (Cl *vs.* I) on Pt. The Cp signals for **6** and **7** appear in their ^1H NMR spectra as singlets at approximately 4.6 ppm. The diastereotopic methylene protons of dppm for each complex display two multiplets with chemical shift differences of about 0.5 ppm.

The spectral data for **8**–**11** are listed in Table 1. Complexes **8** and **9** both exhibit spectra similar to those of complex **3**. In their $^{31}P\{^1H\}$ NMR spectra, two downfield resonances (a doublet and a doublet of doublets) were ascribed to Ru-bound phosphines and one upfield doublet was assigned to Au-bound phosphines. Their ^1H NMR spectra show large differences in the chemical shifts of the diastereotopic methylene protons (3.44 and 3.43 ppm, respectively), indicating the absence of a halide bridge between the two metal centers. The $^{31}P\{^1H\}$ NMR spectrum of complex **10** exhibits two downfield doublets for Ru-bound phosphines and one upfield singlet for Au-bound phosphorus. As expected, the chemical shifts and coupling constants of the Ru-bound phosphorus resonances of **10** are similar to those of the starting material **18**, due to the significant distance between the Ru and Au metal centers. Complex **11** also shows three resonances in the $^{31}P\{^1H\}$ NMR spectrum. All of the phosphorus resonances (Ru-bound and Au-bound) were shifted significantly downfield due to the presence of the $Ph_2PNHPPh_2$ ligand. The N–H proton appears as a multiplet in the ^1H NMR spectrum due to coupling to the adjacent phosphorus atoms.

As expected, three resonances were observed in the $^{31}P\{^1H\}$ NMR spectra of compound **12**. The downfield doublet, which was assigned to Ru-bound PPh_3, appears at a normal chemical shift position (40.3 ppm). The resonance of the Ru-bound bridging dppm phosphorus appears as a doublet of doublets shifted upfield to 26.7 ppm. The furthest upfield broad peak (−18.5 ppm) was assigned to Cu-bound phosphorus.

X-Ray crystallography

Crystallographic details for complexes **4**, **5**, **10** and **12** are provided in Table 2.

Crystal structure of complex 4. Complex **4** exhibits a bridging iodide (Fig. 1, Table 3), with the remaining structure similar to those of its Cl-bridged Ru/Pd and Ru/Pt analogues **1** [11] and **2**.[13] The six central atoms in **4** (Ru1, P2, C6, P3, Pd1, μ-I) form

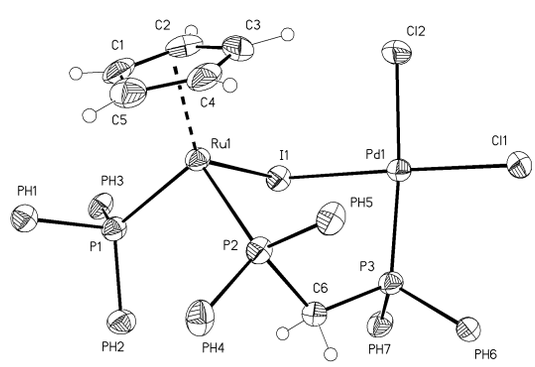

Fig. 1 Thermal ellipsoids drawing of the molecular structure of complex **4**. Thermal ellipsoids are plotted at 50% probability. Phenyl rings and most hydrogen atoms are omitted for clarity.

Table 3 Selected bond distances (Å) and angles (°) for $Cp(PPh_3)Ru(\mu\text{-}I)(\mu\text{-}dppm)PdCl_2$ (**4**)

Ru1–P2	2.3212(12)	Pd1–Cl2	2.3710(12)
Ru1–P1	2.3325(12)	Ru1–I1	2.6749(5)
Pd1–I1	2.5822(5)	Pd1–P3	2.2333(12)
Pd1–Cl1	2.3528(12)		
P2–Ru1–I1	90.70(3)	P3–Pd1–Cl2	174.26(5)
P1–Ru1–I1	91.31(3)	Cl2–Pd1–I1	89.96(3)
P2–Ru1–P1	98.19(4)	C6–P2–Ru1	120.29(15)
Cl1–Pd1–Cl2	90.61(4)	Pd1–I1–Ru1	101.408(16)
P3–Pd1–I1	85.88(3)	C6–P3–Pd1	115.38(14)
Cl1–Pd1–I1	174.85(3)	P3–C6–P2	121.7(2)
P3–Pd1–Cl1	93.88(4)		

Table 4 Selected bond distances (Å) and angles (°) for $Cp(PPh_3)Ru(\mu\text{-}Cl)(\mu\text{-}dppm)Pd(CH_3)Cl$ (**5**)

Ru–P1	2.3282(6)	Pd–P3	2.2208(6)
Ru–Cl1	2.4436(5)	Pd–Cl1	2.4479(5)
Ru–P2	2.3039(6)	Pd–Cl2	2.3843(6)
Pd–C81	2.081(2)		
P2–Ru–Cl1	90.33(2)	P3–Pd–Cl1	87.44(2)
P1–Ru–Cl1	88.314(19)	Cl2–Pd–Cl1	91.90(2)
P2–Ru–P1	98.33(2)	Ru–Cl1–Pd	104.82(2)
C81–Pd–P3	90.09(7)	P2–C6–P3	119.58(12)
C81–Pd–Cl2	90.75(7)	C6–P2–Ru	120.39(7)
P3–Pd–Cl2	177.51(2)	C6–P3–Pd	113.97(7)
C81–Pd–Cl1	175.00(7)		

a distorted six-membered ring with a pseudo-tetrahedral geometry at Ru and square planar structure at Pd. The Ru–I distance in **4**, 2.6749(5) Å, is comparable to the shorter value of 2.685(1) Å reported for $[Ru_2I(CO)_4(C_7H_6Ph)]$, in which the iodide bridges asymmetrically between the two Ru centers.[20] The Pd–I bond length, 2.5822(5) Å, is shorter than the 2.665(1) and 2.723(1) Å distances found in $[(\mu\text{-}I)PdP(o\text{-}tol)_2(o\text{-}C_6H_4\text{-}CH_2)]_2$, in which the Pd–I bond is *trans* to P and C, respectively.[21] The Pd–Cl1 bond of **4** [2.3528(12) Å] is longer than the analogous distance in **1** [2.2842(8) Å] due to the higher *trans* influence of I as compared to Cl.

Crystal structure of complex 5. Complex **5** (Fig. 2, Table 4) is formally the result of replacement of one Pd-bound Cl of **1** with a methyl group *trans* to the chloride bridge. As expected, complexes **1** and **5** exhibit nearly identical structures. The exception is the Pd-(μ-Cl) bond of **5**, 2.4479(5) Å, which is significantly longer than the analogous bond in **1** [2.3256(7) Å] due to the higher *trans* influence of CH_3 as compared to Cl.

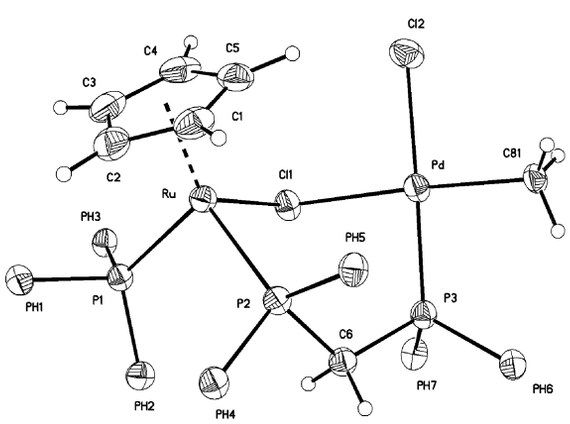

Fig. 2 Thermal ellipsoids drawing of the molecular structure of complex **5**. Thermal ellipsoids are plotted at 50% probability. Phenyl rings and most hydrogen atoms are omitted for clarity.

Crystal structure of complex 10. As shown in Fig. 3, Table 5, complex **10** possesses a dppb linkage between Ru and Au with the three-legged piano-stool geometry at Ru and linear

Table 5 Selected bond distances (Å) and angles (°) for $Cp(PPh_3)RuCl[\mu\text{-}PPh_2(CH_2)_4PPh_2]AuCl$ (**10**)

Ru–P3	2.3000(8)	Au–P1	2.2337(9)
Ru–P2	2.3123(8)	Au–Cl2	2.2759(10)
Ru–Cl1	2.4645(9)		
P3–Ru–P2	96.63(3)	P1–Au–Cl2	176.47(4)
P2–Ru–Cl1	88.42(3)	C7–C6–P2	118.1(2)
P3–Ru–Cl1	95.12(3)	C8–C7–C6	111.0(3)
C6–P2–Ru	117.96(11)	C7–C8–C9	115.7(3)
C9–P1–Au	113.06(11)	C8–C9–P1	113.8(2)

Table 6 Selected bond distances (Å) and angles (°) for $Cp(PPh_3)Ru(\mu\text{-}I)(\mu\text{-}dppm)CuI$ (**12**)

Ru–P2	2.3197(6)	Cu–I1	2.6244(4)
Ru–P3	2.3254(6)	Cu–I2	2.499(3)
Ru–I1	2.7403(2)	Cu–I2′	2.446(4)[a]
Cu–P1	2.2113(8)		
P2–Ru–P3	99.05(2)	P1–Cu–I1	102.23(2)
P2–Ru–I1	94.607(16)	I2′–Cu–I2	8.28(19)
P3–Ru–I1	91.974(15)	Cu–I1–Ru	99.374(10)
P1–Cu–I2	136.63(10)	C6–P2–Ru	122.69(8)
P1–Cu–I2′	137.62(10)	C6–P1–Cu	113.84(8)
I2–Cu–I1	120.83(9)	P1–C6–P2	116.09(14)
I2′–Cu–I1	119.95(9)		

[a] I2′ refers to the alternative position of the disordered I.

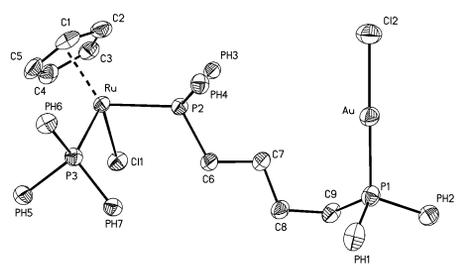

Fig. 3 Thermal ellipsoids drawing of the molecular structure of complex **10**. Thermal ellipsoids are plotted at 50% probability. Phenyl rings and most hydrogen atoms are omitted for clarity.

configuration at Au that were previously reported for the related complex **3**.[11] Due to the long distance between the two metals, their only interactions would be the insignificant perturbations transmitted through the phosphine.

Crystal structure of complex 12. Complex **12** (Fig. 4, Table 6) exhibits a bridging iodide and a distorted six-membered ring formed by the six central atoms (Cu, P1, C6, P2, Ru, μ-I1). The disordered I2 was found in two alternative positions (I2 and I2′) with a I2–Ru–I2′angle of 0.88° and a bond length difference of 0.052 Å between Ru–I2 and Ru–I2′. The standard

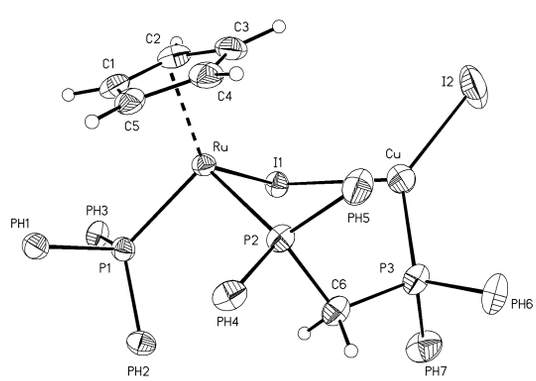

Fig. 4 Thermal ellipsoids drawing of the molecular structure of complex **12**. Thermal ellipsoids are plotted at 50% probability. Phenyl rings and most hydrogen atoms are omitted for clarity.

Table 7 Formal potentials for complexes **1**–**12**[a]

Complex	Couple	E_{pa}/V	$E_{1/2}$[b]/V	Couple	E_{pa}/V	$E_{1/2}$[b]/V	Couple	E_{pa}/V	Ref.
1	Ru(II/III)	1.30		Pd(II/IV)	1.49		Ru(III/IV)	1.92	[c]
1	Ru(II/III)	1.29		Pd(II/IV)	1.45				11
2	Ru(II/III)	1.25	1.21	Pt(II/IV)	1.69		Ru(III/IV)	1.91	[c]
2	Ru(II/III)		1.13[d]	Pt(II/IV)	1.78[d]				12
3	Ru(II/III)	0.95	0.89	Au(I/III)	1.42		Ru(III/IV)	1.81	[c]
3	Ru(II/III)		0.86	Au(I/III)	1.40				11
4	Ru(II/III)	1.29		Pd(II/IV)	1.55	1.50	Ru(III/IV)	1.98	[c]
5	Ru(II/III)	1.13	1.10	Pd(II/IV)	1.50	1.43	Ru(III/IV)	1.95	[c]
6	Ru(II/III)	1.29	1.25	Pt(II/IV)	1.54	1.47	Ru(III/IV)	1.90	[c]
7	Ru(II/III)	1.10		Pt(II/IV)	1.49	1.43	Ru(III/IV)	1.98	[c]
8	Ru(II/III)	0.97	0.89	Au(I/III)	1.54		Ru(III/IV)	1.80	[c]
9	Ru(II/III)	0.95	0.89	Au(I/III)	1.48		Ru(III/IV)	1.85	[c]
10	Ru(II/III)	0.80	0.75	Au(I/III)			Ru(III/IV)	1.76	[c]
11	Ru(II/III)	1.02	0.97	Au(I/III)	1.41		Ru(III/IV)	1.78	[c]
12	Ru(II/III)	1.12		Cu(I/II)	0.88		Ru(III/IV)	1.80	[c]
13	Ru(II/III)		0.61				Ru(III/IV)	1.29	11
14	Ru(II/III)		0.56[d]						12
14	Ru(II/III)	0.85	0.72						[c]
15	Ru(II/III)	0.85	0.73						[c]
16	Ru(II/III)	0.83							[c]
17	Ru(II/III)	0.53							[c]
18	Ru(II/III)	0.80	0.75						[c]
19	Ru(II/III)	0.87	0.76						

[a] All potentials obtained in DCE/TBAT (tetrabutylammonium triflate) unless otherwise specified and reported *vs.* NHE. [b] $E_{1/2}$ reported for reversible waves. [c] This work. [d] Potential obtained in CH_2Cl_2/TBAH (tetrabutylammonium hexafluorophosphate) and reported *vs.* NHE.

pseudo-tetrahedral geometry is observed at Ru while the Cu site exhibits a distorted trigonal-planar geometry with Cu lying slightly out of the I_2P plane (0.075 Å from the I1P1I2 plane and −0.059 Å from the I1P1I2′plane). The I–Cu–P angles of 102.23(2) and 136.63(10)° result from an angular distortion which also occurs in $Cu_2I_2(PPh_3)_3$[22] and $[CuI(PPh_3)]_4$.[23] The Cu–P and Cu–I bond distances of **12** are typical of those found in three-coordinate Cu(I) complexes.[22–25]

Cyclic voltammetry

Voltammetry of complexes 1–12. Cyclic voltammograms of the heterobimetallic complexes **1**–**12** generally exhibit three redox waves within the solvent window (Table 7). The first and the third wave are assigned to the Ru(II/III) and Ru(III/IV) couples, respectively, while the middle one is ascribed to a redox couple of the second metal. The exception is Ru/Cu complex **12**, for which the Cu(I/II) couple at 0.88 V occurs at a less positive potential than the Ru(II/III) wave (*vide infra*). The potentials of the Ru(III/IV) waves vary little among the binuclear complexes but the first oxidation potential of each metal center is dependent on the amount of electron donation from Ru to the second metal center through the bridging ligands.

Significant electron donation from Ru to Pd or Pt through the halide bridge can be seen in all of the Ru/Pd and Ru/Pt bimetallics (**1**, **2**, **4**–**7**) by comparison of their Ru(II/III) redox potentials to those of the model compounds $CpRu(PPh_3)(\eta^1\text{-dppm})Cl$ (**14**) and $CpRu(PPh_3)(\eta^1\text{-dppm})I$ (**16**). All of the bimetallics show significant positive shifts of the Ru(II/III) wave upon introduction of the halide bridge to the second metal. However, the identity of the halide is less critical. Comparison of the I-bridged complexes **4** and **6** with their Cl-bridged analogues **1** and **2** reveals negligible perturbations in the Ru(II/III) or Ru(III/IV) potentials as the bridging halide is changed. More substantial effects can be seen in the Pd(II/IV) and Pt(II/IV) couples. Although these waves are irreversible in Cl-bridged complexes **1** and **2**, compounds **4** and **6** exhibit reversible Pd(II/IV) and Pt(II/IV) waves, respectively, implying greater stability for the oxidized I-bridged complexes. While I-bridged Ru/Pd complex **4** exhibits a positive shift of about 60 mV for the Pd(II/IV) potential as compared to the same wave in **1**, the Pt center of **6** is approximately 150 mV easier to oxidize than the analogous Pt site in **2**.

Interestingly, changing the identity of the ligands on Pd or Pt has its largest effect on the Ru(II/III) redox potentials of analogous complexes. Substituting an electron donating methyl group for a chloride in Ru/Pd complex **1** to yield the Pd–Me species **5** causes the Ru(II/III) wave of **5** to become reversible and shifts its anodic peak potential 170 mV negative of that in **1**. A similar effect is noted for the I-bridged Ru/Pt compound **6** and its Pt–I analogue **7**. In this case, iodide **7** exhibits an approximately 200 mV negative shift for the anodic wave of the Ru(II/III) couple with respect to **6**. For both related pairs (**1** and **5**; **6** and **7**), the Pd or Pt(II/IV) and Ru(III/IV) couples occur at similar potentials.

The Ru/Cu compound **12** exhibits a complex cyclic voltammogram. Two major irreversible waves at 1.12 and 1.80 V were ascribed to the Ru(II/III) and Ru(III/IV) redox couples, respectively. A small wave at 0.88 V, partially overlapping with the Ru(II/III) couple, was assigned as the Cu(I/II) redox couple. This assignment is consistent with the cyclic voltammetry of cyano-bridged Cu(I)–Ru(II) complexes, for which it was reported that Cu(I) was oxidized at less positive potentials than Ru(II).[26,27] The assigned Cu(I/II) redox potential for **12** is also similar to the value of 0.82 V *vs.* NHE (reported as 0.58 V *vs.* SCE) for the model compound $[Cu(dppm)I]_2$.[28] Subsequent scans resulted in the presence of an additional small shoulder peak at 1.25 V, which can be attributed to halide dissociation and formation of a solvent-coordinated species, as has previously been observed in cyclic voltammograms of Cu(I) iodide complexes.[29]

The dppm-bridged Ru/Au bimetallic complexes **3**, **8**, **9** exhibit reversible waves for the Ru(II/III) couple and irreversible waves for the Au(I/III) couple. The redox potentials for both the Ru(II/III) and Au(I/III) couples are close to those of their mononuclear model compounds, indicating minimal electronic communication between the two metal centers through the dppm bridge. Interestingly, changing the halides from Cl to Br to I on the Ru center did not affect the formal potential of the Ru(II/III) couple (0.89 V for all three complexes **3**, **8**, **9**), while the anodic peak potentials of the Au(I/III) couple were shifted slightly positive as the halide went from Cl to Br to I.

The dppb-bridged Ru/Au compound **10** exhibits a reversible couple at 0.75 V and an irreversible couple at 1.76 V *vs.* NHE, which were attributed to the Ru(II/III) and Ru(III/IV) couples, respectively. Under the original conditions of the cyclic voltammetry experiment, the Au(I/III) couple could not be observed. In comparison, the Au (I/III) wave of the dppm-bridged analogue **3** can be observed at 1.40 V.[11] It was possible that the Au(I/III) wave was obscured by the Ru(III/IV) couple at 1.76 V, since the starting material, $Au(PPh_3)Cl$, has been reported to oxidize at 1.68 V *vs.* NHE in CH_2Cl_2.[30] Another possibility was that the Au(I/III) wave was not evident due to a lack of suitable ligands in the electrolyte solution for the incipient Au(III) complex. The electrochemistry of $Au(PR_3)Cl$ complexes is complicated by substitutional equilibria involving phosphine and halide ligands.[31,32] In order to investigate this possibility, the cyclic voltammetry of **10** was investigated in the presence of Bu_4NCl as a chloride source. Under these conditions, a broad shoulder peak was observed on the less positive side of the Ru(III/IV) wave. Although the peak potential could not be accurately determined, the appearance of this wave in the presence of Cl^- is consistent with the need for a ligand in solution for the peak to be observed.

The negligible interaction between the Ru and Au centers in **10** is evidenced by the lack of a shift in the Ru(II/III) couple between the starting material $CpRu(PPh_3)(\eta^1\text{-dppb})Cl$ (**18**) and Ru/Au complex **10** (0.75 V for both). Note that the Ru/Au compound **3**, in which the centers are bridged by the smaller dppm ligand, exhibits a 100 mV shift in the anodic Ru(II/III) wave when the Au center is coordinated to the starting material $CpRu(PPh_3)(\eta^1\text{-dppm})Cl$.[11] Overall, the Ru(II/III) and Ru(III/IV) redox couples of complex **10** more closely resemble the mononuclear model compound due to the longer bridge between the two metal centers.

The cyclic voltammogram of the Ru/Au complex **11** shows a reversible Ru(II/III) couple shifted 210 mV positive as compared to the same wave in the mononuclear complex **19**, providing evidence of electron donation from Ru through the $Ph_2PNH\text{-}PPh_2$ bridge.

UV/vis spectroscopy

In order to investigate the effects of changes in the metal and ancillary ligands on the electronic structure of the bimetallic complexes, the absorption spectra of complexes **1**–**19** were measured in methylene chloride solution (Table 8). For the mononuclear complexes **13**–**16**, **18**–**19** and the Ru/Au bimetallics **3**, **8**–**11**, a weak low energy band at 440–470 nm (band I, Fig. 5) is accompanied by a pair of overlapping bands at higher energy (bands II and III, Fig. 5). By analogy to the known compounds $Cp^*(PMe_3)_2RuX$,[33] we have assigned these transitions as Ru d–d bands. The relatively low extinction coefficients and lack of solvatochromism as the solvent polarity varies from benzene to DMSO support this assignment. Note also the red shift in band III as the halide goes from Cl to Br to I in the series **14**–**16**. An analogous effect was seen as the ligand field strength of X decreased in the series $Cp^*(PMe_3)_2RuX$.[33] The nearly identical absorption spectra of Ru complexes **13**–**19** and the Ru/Au bimetallics **3**, **8**–**11** suggest negligible electronic interaction between the metal centers, a conclusion consistent with the results of cyclic voltammetry.

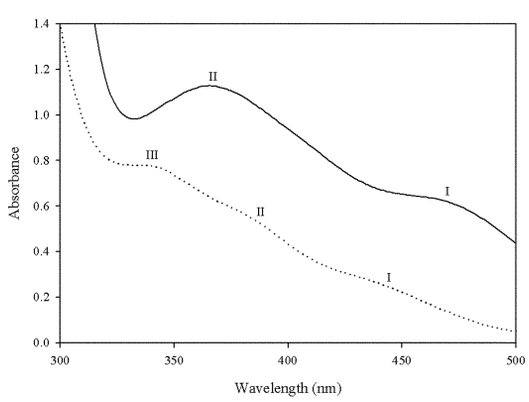

Fig. 5 UV/vis absorption spectra of compounds **1** and **3** obtained in THF at room temperature: **1** (—), **3** (· · ·).

Table 8 Absorption data for complexes **1**–**19**[a]

	λ_{max}/nm (ε/M^{-1} cm^{-1})		
Complex	III	II	I
1		365 (3620)	470 (2080)
2	331 (3340)	365 (2750)	
3	336 (2720)	380 (1990)	437 (960)
4		373 (4550)	453 (5030)
5	320 (3940)	372 (1850)	430 (830)
6		354 (6050)	
7		373 (6100)	424 (4030)
8	350 (2670)	380 (2220)	440 (890)
9	343 (2660)	380 (2100)	439 (850)
10	336 (2370)	380 (1730)	436 (830)
11	343 (2460)	370 (1990)	435 (740)
12		380 (2120)	448 (700)
13	321 (2460)	395 (1530)	460 (890)
14	336 (2620)	380 (1990)	436 (930)
15	343 (2606)	380 (2105)	438 (890)
16	350 (2580)	380 (2240)	440 (810)
17	358 (2450)		
18	336 (2310)	380 (1680)	436 (760)
19	338 (2230)	370 (2005)	435 (780)

[a] UV/vis spectra were measured in CH_2Cl_2 at room temperature.

The Ru/Pd, Ru/Pt and Ru/Cu bimetallic complexes (with the exception of **5**) tend to exhibit a simpler band structure with two absorptions of roughly equal intensity (Fig. 5, Table 8). The general similarity of the spectral features of the bimetallic complexes to those of their mononuclear Ru counterparts **13**–**19** imply that the transitions are primarily localized at the Ru center, with the differences in absorption attributed to electronic interactions between Ru and the second metal in the bimetallics.

Conclusions

A series of Ru/Pd, Ru/Pt, Ru/Au and Ru/Cu heterobimetallic complexes with bidentate phosphine bridges has been synthesized and characterized. In addition to the phosphine linker, the Ru/Pd, Ru/Pt and Ru/Cu complexes contain halide bridges that facilitate electronic interactions between the metal centers. The solid-state structures of four of these complexes were determined by X-ray crystallography and were found to be similar to those of previously synthesized related Ru/Pd, Ru/Pt and Ru/Au heterobimetallic complexes.[11,13] Cyclic voltammetry of the halide-bridged complexes revealed shifted redox potentials for the Ru(II/III) couples and the first oxidative wave of the second metal, as compared to mononuclear model compounds. The shifts are consistent with electron donation between the metals through the halide bridge. The Ru/Au complexes **3**, **8**–**11**, which are bridged only by the bidentate phosphine, exhibited minimal electronic effects between the metal centers. The limited interaction between the Ru and Au centers is corroborated by UV/vis spectroscopy, where **3**, **8**–**11** exhibited the band structure characteristic of the Ru mononuclear model compounds **13**–**19**. Studies of the electrochemical oxidation of alcohols with these newly synthesized heterobimetallic complexes are underway.

Experimental

General

Standard Schlenk/vacuum techniques were used throughout. Hexanes, benzene and pentane were distilled from Na/benzophenone ketyl. Methylene chloride and 1,2-dichloroethane were distilled from CaH_2. All NMR solvents were degassed *via* freeze–pump–thaw cycles and stored over molecular sieves. ^1H and ^{31}P NMR spectra were recorded on a Varian VXR 300 or a Varian Mercury 300 NMR spectrometer. ^1H and ^{31}P NMR spectra are referenced to the residual proton in the deuterated solvent and to 85% H_3PO_4, respectively. The ^{31}P NMR spectra were proton-decoupled. High-resolution mass spectrometry was performed by the University of Florida analytical service. Elemental analyses were performed by Robertson Microlit Laboratories, Madison, NJ. UV-visible absorption spectra were recorded on a UV-2501PC-Shimadzu spectrophotometer. $CpRu(PPh_3)_2Cl$,[34,35] $CpRu(PPh_3)_2Me$,[36,37] $CpRu(\eta^2$-dppm)-Cl (**13**),[18] $Cp(PPh_3)Ru(\eta^1$-dppm)Cl (**14**),[19] $Cp(PPh_3)Ru(\mu$-Cl)-(μ-dppm)$PdCl_2$ (**1**),[11] $Cp(PPh_3)Ru(\mu$-Cl)(μ-dppm)$PtCl_2$ (**2**)[13] and $Cp(PPh_3)RuCl(\mu$-dppm)AuCl (**3**)[11] were prepared as previously described. All other starting materials were purchased in reagent grade purity and used without further purification.

Electrochemistry

Electrochemical experiments were performed under nitrogen using an EG&G PAR model 263A potentiostat/galvanostat. Cyclic voltammograms (scan rate = 50 mV s^{-1}) were recorded in 3.5 ml of DCE/0.7 M TBAT at ambient temperature under nitrogen. All potentials are reported *vs.* NHE and referenced to Ag/Ag^+. The reference electrode consisted of a silver wire immersed in an acetonitrile solution containing freshly prepared 0.01 M $AgNO_3$ and 0.1 M TBAT. The Ag^+ solution and silver wire were contained in a 75 mm glass tube fitted at the bottom with a Vycor tip. All electrochemical measurements were performed inside a glove box. Cyclic voltammetry was performed with a highly polished glassy-carbon working electrode (3 mm diameter).

Synthesis

$CpRu(PPh_3)_2I$. In a 100 ml Schlenk flask, $CpRu(PPh_3)_2Cl$ (0.725 g, 1.00 mmol) and NaI (3.00 g, 20.0 mmol) were dissolved in 60 ml of degassed methanol. The cloudy mixture was stirred at room temperature for 3 days. The red precipitate was filtered out and dissolved in 20 ml of CH_2Cl_2. The solution was washed with water (20 ml × 2), dried over anhydrous $MgSO_4$. Removal of the solvent afforded the red product. Yield: 0.776 g (95%). The compound was identified by comparison to literature data.[36]

$CpRu(PPh_3)_2Br$. The reaction was performed similarly as for $CpRu(PPh_3)_2I$ starting from $CpRu(PPh_3)_2Cl$ (0.725 g, 1.00 mmol) and LiBr (1.30 g, 15.0 mmol). Yield: 0.724 g (94%). The compound was identified by comparison to literature data.[38]

$CpRu(PPh_3)(\eta^1$-dppm)Br (15). In a 50 ml Schlenk flask, $CpRu(PPh_3)_2Br$ (0.500 g, 0.649 mmol) and dppm (0.264 g, 0.688 mmol) were dissolved in 30 ml of benzene. The yellow solution was heated to 65 °C and stirred for 6 h, during which an orange precipitate formed. The mixture was cooled to room temperature and filtered to afford **15** as an orange powder. Yield: 0.527 g (91%). ^1H NMR ($CDCl_3$): δ 7.82–6.95 (m, 35H, $Ph_2PCH_2PPh_2$ + PPh_3), 4.13 (s, 5H, Cp), 3.94 (m, 1H, $Ph_2PCHHPPh_2$), 1.15 (m, 1H, $Ph_2PCHHPPh_2$). ^{31}P NMR ($CDCl_3$): δ 43.2 (d, Ru–PPh_3, J_{PP} = 42 Hz), 35.8 (dd, Ru–$Ph_2PCH_2PPh_2$, J_{PP} = 42, 20 Hz), −27.5 (d, Ru–$Ph_2PCH_2PPh_2$, J_{PP} = 20 Hz). HRMS (FAB): calc. for $C_{48}H_{42}P_3Ru$ *m/z* 813.1549 $(M - Br)^+$, found 813.1545.

$CpRu(PPh_3)(\eta^1$-dppm)I (16). The reaction was performed similarly as for **15** starting from $CpRu(PPh_3)_2I$ (0.500 g, 0.612 mmol) and dppm (0.250 g, 0.650 mmol). Yield: 0.518 g (90%). ^1H NMR ($CDCl_3$): δ 7.86–6.94 (m, 35H, $Ph_2PCH_2PPh_2$ + PPh_3), 4.18 (s, 5H, Cp), 4.12 (m, 1H, $Ph_2PCHHPPh_2$), 1.24 (m, 1H, $Ph_2PCHHPPh_2$). ^{31}P NMR ($CDCl_3$): δ 42.9 (d, Ru–PPh_3, J_{PP} = 41 Hz), 33.5 (dd, Ru–$Ph_2PCH_2PPh_2$, J_{PP} = 41, 20 Hz), −27.0 (d, Ru–$Ph_2PCH_2PPh_2$, J_{PP} = 20 Hz). HRMS (FAB): calc. for $C_{48}H_{42}P_3Ru$ *m/z* 813.1549 $(M - I)^+$, found 813.1541.

$CpRu(PPh_3)(\eta^1$-dppm)Me (17). In a 100 ml Schlenk flask, $CpRu(PPh_3)_2Me$ (0.500 g, 0.709 mmol) and dppm (0.544 g, 1.42 mmol) were dissolved in 50 ml of benzene. The orange–brown solution was heated to 80 °C and stirred for 5 days. The mixture was cooled to room temperature and the solvent was removed under vacuum to produce a brown residue which was recrystallized in CH_2Cl_2–pentane to afford the yellow product. Yield: 0.381 g (65%). ^1H NMR ($CDCl_3$): δ 7.40–6.85 (m, 35H, $Ph_2PCH_2PPh_2$ + PPh_3), 4.19 (s, 5H, Cp), 2.82 (m, 1H, $Ph_2PCHHPPh_2$), 1.15 (m, 1H, $Ph_2PCHHPPh_2$), 0.37 (t, 3H, CH_3, J_{PH} = 6 Hz). ^{31}P NMR ($CDCl_3$): δ 59.3 (d, Ru–PPh_3, J_{PP} = 3, 37 Hz), 48.2 (dd, Ru–$Ph_2PCH_2PPh_2$, J_{PP} = 16, 37 Hz), −27.8 (d, Ru–$Ph_2PCH_2PPh_2$, J_{PP} = 3, 16 Hz). HRMS (FAB): calc. for $C_{48}H_{42}P_3Ru$ *m/z* 813.1549 $(M - CH_3)^+$, found 813.1537.

$CpRu(PPh_3)(\eta^1$-dppb)Cl (18). In a 50 ml Schlenk flask, $CpRu(PPh_3)_2Cl$ (1.000 g, 1.378 mmol) and dppb (0.705 g, 1.65 mmol) were dissolved in 30 ml of CH_2Cl_2. The yellow solution was kept refluxing for 3 days. The mixture was cooled to room temperature and condensed to a small volume (~5 ml). Pentane (30 ml) was added to precipitate the yellow powder, which was filtered off and dried under vacuum. The resulting solid was purified by chromatography on Al_2O_3 (2.5 × 10 cm) with 1 : 3 hexane–ether as eluent. Yield: 0.74 g (60%). ^1H NMR ($CDCl_3$): δ 7.88–6.98 (m, 35H, $Ph_2P(CH_2)_4PPh_2$ + PPh_3), 4.09 (s, 5H, Cp), 2.30–0.50 (m, 8H, $Ph_2P(CH_2)_4PPh_2$). ^{31}P NMR ($CDCl_3$): δ 44.7 (d, Ru–PPh_3, J_{PP} = 42 Hz), 37.3 (d, Ru–Ph_2P-$(CH_2)_4PPh_2$, J_{PP} = 42 Hz), −14.4 (s, Ru–$Ph_2P(CH_2)_4PPh_2$). HRMS (FAB): calc. for $C_{51}H_{48}P_3ClRu$ *m/z* 890.1704 (M^+), found 890.1716.

$CpRu(PPh_3)(\eta^1$-$Ph_2PNHPPh_2)Cl$ (19). The reaction was performed similarly as for **15** starting from $CpRu(PPh_3)_2Cl$ (0.500 g, 0.689 mmol) and $Ph_2PNHPPh_2$ (0.278 g, 0.724 mmol). Yield: 0.538 g (92%). ^1H NMR ($CDCl_3$): δ 7.82–6.97 (m, 35H, $Ph_2PNHPPh_2$ + PPh_3), 4.82 (m, 1H, $Ph_2PNHPPh_2$), 4.11 (s, 5H, Cp). ^{31}P NMR ($CDCl_3$): δ 85.5 (dd, Ru–$Ph_2PNHPPh_2$, J_{PP} = 46, 12 Hz), 42.0 (d, Ru–PPh_3, J_{PP} = 46 Hz), 24.3 (d, Ru–$Ph_2PNHPPh_2$, J_{PP} = 12 Hz). HRMS (FAB): calc. for $C_{47}H_{41}NClP_3Ru$ *m/z* 814.1489 $(M - Cl)^+$, found 814.1465.

$Cp(PPh_3)Ru(\mu$-I)(μ-dppm)$PdCl_2$ (4). In a 25 ml Schlenk flask, $CpRu(PPh_3)(\eta^1$-dppm)I (0.200 g, 0.213 mmol) and Pd(COD)Cl_2 (0.061 g, 0.21 mmol) were dissolved in 10 ml of CH_2Cl_2. The red–orange solution was stirred at room temperature overnight. The solution was condensed under vacuum to a small volume (~3 ml), and pentane (15 ml) was transferred through a syringe to precipitate a red solid. The solid was filtered with a medium swivel frit, washed with hexanes, and dried under vacuum. The product was recrystallized from CH_2Cl_2–pentane to yield 0.202 g (84.9%). Single crystals suitable for X-ray diffraction were grown by slow solvent diffusion of pentane into a solution of **4** in chloroform. ^1H NMR ($CDCl_3$): δ 8.08–6.16 (m, 35H, $Ph_2PCH_2PPh_2$ + PPh_3), 4.65 (s, 5H, Cp), 3.48 (m, 1H, $Ph_2PCHHPPh_2$), 2.72 (m, 1H, $Ph_2PCHHPPh_2$). ^{31}P NMR ($CDCl_3$): δ 49.5 (dd, Ru–$Ph_2PCH_2PPh_2$, J_{PP} = 20 Hz, 35 Hz), 40.1 (dd, Ru–PPh_3, J_{PP} = 7, 35 Hz), 10.5 (dd, $Ph_2PCH_2PPh_2$–Pd, J_{PP} = 7, 20 Hz). HRMS (FAB): calc. for $C_{48}H_{42}IClP_3PdRu$ *m/z* 1080.9312 $(M - Cl)^+$, found 1080.9304. Anal. Calc. for

$C_{48}H_{42}Cl_2IP_3PdRu$: C, 51.66; H, 3.70. Found: C, 51.36; H, 3.52%.

Cp(PPh$_3$)Ru(μ-Cl)(μ-dppm)Pd(CH$_3$)Cl (5). In a 25 ml Schlenk flask, CpRu(PPh$_3$)(η^1-dppm)Me (0.200 g, 0.242 mmol) and Pd(COD)Cl$_2$ (0.069 g, 0.24 mmol) were dissolved in 10 ml of benzene. The clear solution was stirred at room temperature for 4 h, during which a precipitate formed. The solid was filtered with a frit, washed with pentane, and dried under vacuum. Yield: 0.224 g (92%). Single crystals suitable for X-ray diffraction were grown by slow diffusion of pentane into a solution of the orange product **5** in 1,2-dichloroethane. ^{1}H NMR ($CDCl_3$): δ 8.06–5.90 (m, 35H, $Ph_2PCH_2PPh_2$ + PPh_3), 4.58 (s, 5H, Cp), 2.86 (m, 2H, $Ph_2PCH_2PPh_2$), 0.39 (d, 3H, CH_3, J_{PH} = 3 Hz). ^{31}P NMR ($CDCl_3$): δ 45.6 (dd, Ru–$Ph_2PCH_2PPh_2$, J_{PP} = 36, 27 Hz), 39.3 (d, Ru–PPh_3, J_{PP} = 36 Hz), 25.5 (d, $Ph_2PCH_2PPh_2$–Pd, J_{PP} = 27 Hz). HRMS (FAB): calc. for $C_{49}H_{45}P_3ClRuPd$ *m*/*z* 969.0501 (M − Cl)$^+$, found 969.0494. Anal. Calc. for $C_{49}H_{45}Cl_2P_3PdRu$: C, 58.57; H, 4.42. Found: C, 57.86; H, 3.94%.

Cp(PPh$_3$)Ru(μ-I)(μ-dppm)PtCl$_2$ (6). The reaction was performed similarly as for **4** starting from CpRu(PPh$_3$)(η^1-dppm)I (0.200 g, 0.213 mmol) and Pt(COD)Cl$_2$ (0.080 g, 0.21 mmol). Yield: 0.188 g (73%). ^{1}H NMR ($CDCl_3$): δ 8.04–6.12 (m, 35H, $Ph_2PCH_2PPh_2$ + PPh_3), 4.63 (s, 5H, Cp), 3.45 (m, 1H, $Ph_2PCHHPPh_2$), 2.94 (m, 1H, $Ph_2PCHPPh_2$). ^{31}P NMR ($CDCl_3$): δ 46.4 (dd, Ru–$Ph_2PCH_2PPh_2$, J_{PP} = 11, 35 Hz), 40.5 (d, Ru–PPh_3, J_{PP} = 3, 35 Hz), −7.7 (d, $Ph_2PCH_2PPh_2$–Pt, J_{PP} = 3, 11 Hz). HRMS (FAB): calc. for $C_{48}H_{42}IClP_3PtRu$ *m*/*z* 1169.9924 (M − Cl)$^+$, found 1169.9916. Anal. Calc. for $C_{48}H_{42}Cl_2IP_3PtRu$: C, 47.82; H, 3.51. Found: C, 47.60; H, 3.36%.

Cp(PPh$_3$)Ru(μ-I)(μ-dppm)PtI$_2$ (7). The reaction was performed similarly as for **4** starting from CpRu(PPh$_3$)(η^1-dppm)I (0.200 g, 0.213 mmol) and Pt(COD)I$_2$ (0.119 g, 0.213 mmol). Yield: 0.266 g (90%). ^{1}H NMR ($CDCl_3$): δ 8.12–5.76 (m, 35H, $Ph_2PCH_2PPh_2$ + PPh_3), 4.65 (s, 5H, Cp), 3.52 (m, 1H, $Ph_2PCHHPPh_2$), 3.12 (m, 1H, $Ph_2PCHHPPh_2$). ^{31}P NMR ($CDCl_3$): δ 45.8 (dd, Ru–$Ph_2PCH_2PPh_2$, J_{PP} = 12 Hz, 35 Hz), 40.4 (dd, Ru–PPh_3, J_{PP} = 3, 35 Hz), −2.1 (dd, $Ph_2PCH_2PPh_2$–Pt, J_{PP} = 3, 12 Hz). HRMS (FAB): calc. for $C_{48}H_{42}I_3P_3PtRu$ *m*/*z* 1261.9280 (M − I)$^+$, found 1261.9274. Anal. Calc. for $C_{48}H_{42}I_3P_3PtRu$: C, 41.52; H, 3.05. Found: C, 41.24; H, 2.79%.

Cp(PPh$_3$)RuI(μ-dppm)AuI (8). In a 20 ml Schlenk flask, CpRu(PPh$_3$)(η^1-dppm)I (0.200 g, 0.213 mmol) and AuI (0.069 g, 0.213 mmol) were slurried in 10 ml of CH_2Cl_2. The mixture was stirred at room temperature for 5 h, during which the solid AuI dissolved to afford a clear orange–red solution. The solution was condensed under vacuum to a small volume (~3 ml), and hexane (15 ml) was transferred through a syringe to precipitate a red solid. The solid was filtered with a medium swivel frit, washed with hexanes, and dried under vacuum. Yield: 0.260 g (97%). ^{1}H NMR ($CDCl_3$): δ 8.07–6.13 (m, 35H, $Ph_2PCH_2PPh_2$ + PPh_3), 5.04 (m, 1H, $Ph_2PCHHPPh_2$), 4.16 (s, 5H, Cp), 1.60 (m, 1H, $Ph_2PCHHPPh_2$). ^{31}P NMR ($CDCl_3$): δ 41.7 (d, Ru–PPh_3, J_{PP} = 42 Hz), 31.4 (dd, Ru–$Ph_2PCH_2PPh_2$, J_{PP} = 42, 25 Hz), 27.9 (d, $Ph_2PCH_2PPh_2$–Au, J_{PP} = 25 Hz). HRMS (FAB): calc. for $C_{48}H_{42}P_3I_2RuAu$ *m*/*z* 1137.0255 (M − I)$^+$, found 1137.0246. Anal. Calc. for $C_{48}H_{42}P_3I_2RuAu$: C, 45.63; H, 3.35. Found: C, 45.70; H, 3.36%.

Cp(PPh$_3$)RuBr(μ-dppm)AuCl (9). The reaction was performed similarly as for **3**[11] starting from CpRu(PPh$_3$)(η^1-dppm)Br (0.200 g, 0.224 mmol) and Au(PPh$_3$)Cl (0.111 g, 0.224 mmol). Yield: 0.179 g (71.0%). ^{1}H NMR ($CDCl_3$): δ 7.96–6.86 (m, 35H, $Ph_2PCH_2PPh_2$ + PPh_3), 4.86 (m, 1H, $Ph_2PCHHPPh_2$), 4.12 (s, 5H, Cp), 1.43 (m, 1H, $Ph_2PCHHPPh_2$). ^{31}P NMR ($CDCl_3$): δ 42.5 (d, PPh_3–Ru, J_{PP} = 42 Hz), 34.2 (dd, Ru–$Ph_2PCH_2PPh_2$, J_{PP} = 42, 28 Hz), 22.0 (d, $Ph_2PCH_2PPh_2$–Au, J_{PP} = 28 Hz). HRMS (FAB): calc. for $C_{48}H_{42}P_3BrClRuAu$ *m*/*z* 1089.0392 (M − Cl)$^+$, found 1089.0398. Anal. Calc. for $C_{48}H_{42}P_3BrClRuAu$: C, 51.24; H, 3.76. Found: C, 51.49; H, 3.67%.

Cp(PPh$_3$)RuCl[μ-PPh$_2$(CH$_2$)$_4$PPh$_2$]AuCl (10). The reaction was performed similarly as for **8** starting from CpRu(PPh$_3$)(η^1-dppb)Cl (0.200 g, 0.224 mmol) and AuCl (0.052 g, 0.224 mmol). Yield: 0.202 g (94%). Single crystals suitable for X-ray diffraction were grown by slow diffusion of pentane into a solution of the yellow product **10** in dichloromethane. ^{1}H NMR ($CDCl_3$): δ 7.84–7.00 (m, 35H, $Ph_2P(CH_2)_4PPh_2$ + PPh_3), 4.11 (s, 5H, Cp), 2.12 (m, 3H, dppb), 1.18 (m, 3H, dppb), 0.58 (m, 2H, dppb). ^{31}P NMR ($CDCl_3$): δ 44.8 (d, PPh_3–Ru, J_{PP} = 42 Hz), 37.0 (d, Ru–$Ph_2P(CH_2)_4PPh_2$, J_{PP} = 42 Hz), 31.6 (s, $Ph_2P(CH_2)_4PPh_2$–Au). HRMS (FAB): calc. for $C_{51}H_{48}P_3Cl_2RuAu$ *m*/*z* 1122.1055 (M$^+$), found 1122.1055. Anal. Calc. for $C_{51}H_{48}P_3Cl_2RuAu$: C, 54.56; H, 4.31. Found: C, 54.30; H, 4.02%.

Cp(PPh$_3$)RuCl(μ-Ph$_2$PNHPPh$_2$)AuCl (11). The reaction was performed similarly as for **8** starting from CpRu(PPh$_3$)(η^1-$Ph_2PNHPPh_2$)Cl (0.200 g, 0.235 mmol) and AuCl (0.0546 g, 0.235 mmol). Yield: 0.208 g (81.6%). ^{1}H NMR ($CDCl_3$): δ 7.93–6.91 (m, 35H, $Ph_2PCH_2PPh_2$ + PPh_3), 5.93 (m, 1H, $Ph_2PNHPPh_2$), 4.12 (s, 5H, Cp). ^{31}P NMR ($CDCl_3$): δ 87.7 (dd, Ru–$Ph_2PNHPPh_2$, J_{PP} = 46, 38 Hz), 54.0 (d, PPh_3–Ru, J_{PP} = 38 Hz), 40.4 (d, $Ph_2PNHPPh_2$–Au, J_{PP} = 46 Hz). HRMS (FAB): calc. for $C_{47}H_{41}NCl_2P_3RuAu$ *m*/*z* 1046.0850 (M − Cl)$^+$, found 1046.0876. Anal. Calc. for $C_{48}H_{42}P_3I_2RuAu$: C, 52.19; H, 3.82; N, 1.29. Found: C, 51.71; H, 3.52; N, 1.21%.

Cp(PPh$_3$)Ru(μ-I)(μ-dppm)CuI (12). In a 25 ml flask, CpRu(PPh$_3$)(η^1-dppm)I (0.200 g, 0.213 mmol) and CuI (0.203 g, 1.07 mmol) were dissolved in 10 ml of CH_2Cl_2. The red cloudy mixture was stirred at room temperature overnight. After the solids settled, the clear red supernatant was transferred to another 25 ml Schlenk flask under N_2 by means of a filter cannula. The filtrate was condensed under vacuum to a small volume (~2 ml), and pentane (15 ml) was added through a syringe to precipitate a red solid. The solid was filtered with a medium swivel frit, washed with pentane (10 ml × 3), and dried under vacuum. Yield: 0.216 g (90%). Single crystals suitable for X-ray diffraction were grown by slow diffusion of pentane into a solution of the red product **12** in dichloromethane. ^{1}H NMR ($CDCl_3$): δ 7.63–6.92 (m, 35H, $Ph_2PCH_2PPh_2$ + PPh_3), 4.34 (s, 5H, Cp), 2.89 (m, 1H, $Ph_2PCHHPPh_2$), 2.51 (m, 1H, $Ph_2PCHHPPh_2$) ^{31}P NMR ($CDCl_3$): δ 40.3 (d, Ru–PPh_3 J_{PP} = 40 Hz), 26.7 (dd, Ru–$Ph_2PCH_2PPh_2$, J_{PP} = 40, 20 Hz), −18.5 (br s, $Ph_2PCH_2PPh_2$–Cu). HRMS (FAB): calc. for $C_{48}H_{42}P_3I_2RuCu$ *m*/*z* 1129.8928 (M$^+$) found 1129.8922. Anal. Calc. for $C_{48}H_{42}P_3I_2RuCu$: C, 51.01; H, 3.75. Found: C, 51.25; H, 3.54%.

X-Ray crystallography

Crystallographic structure determination of complexes 4, 5, 10 and 12. Data for all four complexes were collected at 173 K on a Siemens SMART PLATFORM equipped with a CCD area detector and a graphite monochromator utilizing Mo-Kα radiation (λ = 0.71073 Å). Cell parameters for each structure were refined using up to 8192 reflections. A full sphere of data (1850 frames) was collected using the ω-scan method (0.3° frame width). The first 50 frames were remeasured at the end of data collection to monitor instrument and crystal stability (maximum correction on I was <1%). Absorption corrections by integration were applied based on measured indexed crystal faces. The structures were solved by direct methods in SHELXTL,[39] and refined using full-matrix least squares. The non-H atoms were treated anisotropically, whereas the hydrogen atoms were calculated in ideal positions and were

riding on their respective carbon atoms. All software and sources of the scattering factors are contained in the SHELXTL program library.

For **4**: The asymmetric unit consists of the metal complex and four chloroform molecules. Two of the latter were disordered. For one of these, the whole molecule was refined in two parts with their site occupation factors dependently refined (0.53(1) and 0.47(1) for the major and minor parts, respectively. The second chloroform molecule has its chlorine atoms disordered and was refined in two sets of three (0.57(1) and 0.43(1), respectively). A total of 689 parameters were refined in the final cycle of refinement using 26139 reflections with $I > 2\sigma(I)$ to yield R_1 and wR_2 of 4.62 and 12.33%, respectively. Refinement was done using F^2.

For **5**: The asymmetric unit consists of the complex and three dichloroethane molecules of crystallization. The latter were significantly disordered and could not be fully modeled. Thus the program SQUEEZE,[40] a part of the PLATON[41] package of crystallographic software, was used to calculate the solvent disorder area and remove its contribution to the overall intensity data. A total of 505 parameters were refined in the final cycle of refinement using 9978 reflections with $I > 2\sigma(I)$ to yield R_1 and wR_2 of 2.99 and 7.74%, respectively. Refinement was done using F^2.

For **10**: The AuCl and the two phenyl rings are positionally disordered. Only the AuCl moiety was resolved and was refined in three parts. Their site occupation factors were dependently refined to 0.960(1) for the major part and 0.030(1) for each of the other two parts. A total of 538 parameters were refined in the final cycle of refinement using 8550 reflections with $I > 2\sigma(I)$ to yield R_1 and wR_2 of 2.81 and 7.01%, respectively. Refinement was done using F^2.

For **12**: The asymmetric unit consists of the complex and two molecules of dichloromethane disordered around a center of inversion. The latter could not be fully resolved. Thus the program SQUEEZE,[40] a part of the PLATON[41] package of crystallographic software, was used to calculate the solvent disorder area and remove its contribution to the overall intensity data. A total of 553 parameters were refined in the final cycle of refinement using 9283 reflections with $I > 2\sigma(I)$ to yield R_1 and wR_2 of 2.62 and 7.64%, respectively. Refinement was done using F^2.

CCDC reference numbers 215180–215183.

See http://www.rsc.org/suppdata/dt/b3/b307990b/ for crystallographic data in CIF or other electronic format.

Acknowledgements

The Division of Chemical Sciences, Office of Basic Energy Sciences, U.S. Department of Energy provided partial support of this work. K. A. A. wishes to acknowledge the National Science Foundation and the University of Florida for funding of the purchase of the X-ray equipment.

References

1 D. G. McCollum and B. Bosnich, *Inorg. Chim. Acta*, 1998, **270**, 13.
2 P. Kalck and N. Wheatley, *Chem. Rev.*, 1999, **99**, 3379.
3 E. K. Van Den Beuken and B. L. Feringa, *Tetrahedron*, 1998, **54**, 12985.
4 P. A. Shapley, N. J. Zhang, J. L. Allen, D. H. Pool and H. C. Liang, *J. Am. Chem. Soc.*, 2000, **122**, 1079.
5 K. Severin, *Chem.–Eur. J.*, 2002, **8**, 1514.
6 P. Braunstein and J. Rose, *Met. Cluster Chem.*, 1999, **2**, 616.
7 D. W. Stephan, *Coord. Chem. Rev.*, 1989, **95**, 41.
8 A. M. Baranger and R. G. Bergman, *J. Am. Chem. Soc.*, 1994, **116**, 3822.
9 R. D. Adams and T. S. Barnard, *Organometallics*, 1998, **17**, 2885.
10 J. Xiao and R. J. Puddephatt, *Coord. Chem. Rev.*, 1995, **143**, 457.
11 G. Matare, M. E. Tess, K. A. Abboud, Y. Yang and L. McElwee-White, *Organometallics*, 2002, **21**, 711.
12 S. D. Orth, M. R. Terry, K. A. Abboud, B. Dodson and L. McElwee-White, *Inorg. Chem.*, 1996, **35**, 916.
13 M. E. Tess, P. L. Hill, K. E. Torraca, M. E. Kerr, K. A. Abboud and L. McElwee-White, *Inorg. Chem.*, 2000, **39**, 3942.
14 E. M. Barranco, O. Crespo, M. C. Gimeno, A. Laguna, P. G. Jones and B. Ahrens, *Inorg. Chem.*, 2000, **39**, 680.
15 M. J. Mays and P. A. Vergnano, *J. Chem. Soc., Dalton Trans.*, 1979, 1112.
16 M. C. Gimeno and A. Laguna, *Chem. Rev.*, 1997, **97**, 511.
17 S. Al-Baker, W. E. Hill and C. A. McAuliffe, *J. Chem. Soc., Dalton Trans.*, 1986, 1297.
18 G. S. Ashby, M. I. Bruce, I. B. Tomkins and R. C. Wallis, *Aust. J. Chem.*, 1979, **32**, 1003.
19 M. I. Bruce, M. G. Humphrey, J. M. Patrick and A. H. White, *Aust. J. Chem.*, 1983, **36**, 2065.
20 J. A. K. Howard and P. Woodward, *J. Chem. Soc., Dalton Trans.*, 1977, 366.
21 A. L. Rheingold and W. C. Fultz, *Organometallics*, 1984, **3**, 1414.
22 P. G. Eller, G. J. Kubas and R. R. Ryan, *Inorg. Chem.*, 1977, **16**, 2454.
23 M. R. Churchill, B. G. Deboer and D. J. Donovan, *Inorg. Chem.*, 1975, **14**, 617.
24 G. A. Bowmaker, D. Camp, R. D. Hart, P. C. Healy, B. W. Skelton and A. H. White, *Aust. J. Chem.*, 1992, **45**, 1155.
25 G. A. Bowmaker, J. V. Hanna, R. D. Hart, P. C. Healy and A. H. White, *Aust. J. Chem.*, 1994, **47**, 25.
26 S. Ranjan and S. K. Dikshit, *Transition Met. Chem.*, 2002, **27**, 668.
27 S. Ranjan and S. K. Dikshit, *Polyhedron*, 1998, **17**, 3071.
28 R. Yang, K. Lin, Y. Hou, D. Wang, D. Jin, B. Luo and L. Chen, *Transition Met. Chem.*, 1997, **22**, 254.
29 P. Kulkarni, S. Padhye, E. Sinn, C. E. Anson and A. K. Powell, *Inorg. Chim. Acta*, 2002, **332**, 167.
30 S. Attar, J. H. Nelson, W. H. Bearden, N. W. Alcock, L. Solujic and E. B. Milosavljevic, *Polyhedron*, 1991, **10**, 1939.
31 J. E. Anderson, S. M. Sawtelle and C. E. McAndrews, *Inorg. Chem.*, 1990, **29**, 2627.
32 J. V. McArdle and G. E. Bossard, *J. Chem. Soc., Dalton Trans.*, 1990, 2219.
33 R. G. Bray, J. E. Bercaw, H. B. Gray, M. D. Hopkins and R. A. Paciello, *Organometallics*, 1987, **6**, 922.
34 M. I. Bruce, C. Hameister, A. G. Swincer and R. C. Wallis, *Inorg. Synth.*, 1982, **21**, 78.
35 M. I. Bruce and N. J. Windsor, *Aust. J. Chem.*, 1977, **30**, 1601.
36 T. Blackmore, M. I. Bruce and F. G. A. Stone, *J. Chem. Soc. A*, 1971, 2376.
37 M. I. Bruce, R. C. F. Gardner, J. A. K. Howard, F. G. A. Stone, M. Welling and P. Woodward, *J. Chem. Soc., Dalton Trans.*, 1977, 621.
38 H. Nagashima, K. Yamaguchi, K. Mukai and K. Itoh, *J. Organomet. Chem.*, 1985, **291**, C20.
39 G. M. Sheldrick, in 'SHELXTL program library', Madison, WI, 1998.
40 P. van der Sluis and A. L. Spek, *Acta Crystallogr., Sect. A*, 1990, **46**, 194.
41 A. L. Spek, *Acta Crystallogr., Sect. A*, 1990, **46**, C34.